

Functional Clustering for Longitudinal Associations between Social Determinants of Health and Stroke Mortality in the US

Fangzhi Luo *

Department of Epidemiology and Biostatistics,
College of Public Health, University of Georgia, Athens, GA, USA
Jianbin Tan

Department of Biostatistics and Bioinformatics,
School of Medicine, Duke University, Durham, NC, USA
Donglan Zhang

Department of Foundations of Medicine,
NYU Grossman Long Island School of Medicine, Mineola, NY, USA
Hui Huang

Center for Applied Statistics and School of Statistics,
Renmin University of China, Beijing, China
Ye Shen

Department of Epidemiology and Biostatistics,
College of Public Health, University of Georgia, Athens, GA, USA

June 24, 2024

Abstract

Understanding longitudinally changing associations between Social determinants of health (SDOH) and stroke mortality is crucial for timely stroke management. Previous studies have revealed a significant regional disparity in the SDOH – stroke mortality associations. However, they do not develop data-driven methods based on these longitudinal associations for regional division in stroke control. To fill this gap, we propose a novel clustering method for SDOH – stroke mortality associations in the US counties. To enhance interpretability and statistical efficiency of the clustering outcomes, we introduce a new class of smoothness-sparsity pursued penalties for simultaneous clustering and variable selection in the longitudinal associations. As a result, we can identify important SDOH that contribute to longitudinal changes in the stroke mortality, facilitating clustering of US counties into several regions based on how these SDOH relate to stroke mortality. The effectiveness of our proposed method is demonstrated through extensive numerical studies. By applying our method to a county-level SDOH and stroke mortality longitudinal data, we identify 18 important SDOH for stroke mortality and divide the US counties into two clusters based on these selected SDOH. Our findings unveil complex regional heterogeneity in the longitudinal associations between SDOH and stroke mortality, providing valuable insights in region-specific SDOH adjustments for mitigating stroke mortality.

Keywords: Functional clustering, Mixture model, Variable selection, Regularized expectation-maximization algorithm, Stroke

*Jianbin Tan is the co-first author. The authors gratefully acknowledge *the National Natural Science Foundation of China (grants nos. 12292980, 12292984 and 12231017)* and *the MOE project of key research institute of humanities and social sciences (grant no. 22JJD910001)*.

1 Introduction

The burden of stroke in the United States is enormous. As one of the most prevalent cardiovascular diseases, stroke remains consistently among the top five causes of death in the country (Koton et al., 2014), leading to over 130,000 fatalities annually (Holloway et al., 2014). In the effort to prevent stroke deaths, Social Determinants of Health (SDOH) – encompassing economic, social, and environmental conditions where people live, learn, work, and play (Havranek et al., 2015) – have garnered significant attention due to their strong associations with stroke mortality (Powell-Wiley et al., 2022). Notably, in 2015, the impact of SDOH on stroke mortality was highlighted in an important scientific statement by the American Heart Association (AHA) (Mozaffarian et al., 2015). Furthermore, since 2019, the AHA has consistently emphasized the importance of SDOH in its Annual Heart Disease and Stroke Statistics Report, spanning across all chapters (Benjamin et al., 2019). These declarations underscore the urgency of understanding the associations between SDOH and stroke mortality. This understanding is crucial for informing targeted interventions aimed at controlling stroke mortality by addressing underlying social, economic, and environmental factors.

Recent findings have revealed a clear regional disparity in the associations between SDOH and stroke mortality. For instance, Zelko et al. (2023) identified state-wise differences in these associations. Additionally, Villablanca et al. (2016) and Son et al. (2023) observed significant disparities in the associations between rural and urban areas. To address such regional disparities, various state-wise (Gebreab et al., 2015) and rural-urban strategies (Labarthe et al., 2014; Record et al., 2015; Kapral et al., 2019) have been developed for region-specific stroke management. However, the existing literature does not guarantee that areas within a divided region share similar associations between SDOH and

stroke mortality. Hence, employing a uniform SDOH adjustment in divided regions may not be an effective strategy for preventing stroke disease. Moreover, many SDOH have been found to exhibit longitudinal changes in their associations with stroke mortality (He et al., 2021), a factor crucial for timely policymaking in stroke management. Targeting these longitudinal associations between SDOH and stroke mortality, clustering becomes a vital tool for determining reasonable regional divisions for stroke prevention. Nonetheless, this remains an unsolved issue requiring further investigation.

In this work, we propose a novel method for clustering longitudinal associations between SDOH and stroke mortality. In general, the clustering is implemented based on the similarity among associations from different counties in the US, and the resulting clustering outcomes can then be used to inform region-specific prevention measures for controlling stroke mortality.

To achieve this, we utilize county-level longitudinal data of SDOH and stroke mortality in the US, and treat the longitudinally observed data in each county as functional data. As a result, the concurrent associations between SDOH and stroke mortality are inherently functional objects, which can be effectively modeled using functional regression models, where the coefficients are also functional, capturing the relationship between SDOH and stroke mortality over time. For the clustering process, we model the functional coefficients using a finite mixture model, leading to a finite mixture of functional regression models. This approach enables the clustering of counties in the US into different regions based on the relationship between their SDOH and stroke mortality.

Our task essentially differs from the common clustering procedures for longitudinal data (Jacques and Preda, 2013, 2014; Liang et al., 2021), which primarily apply to observable longitudinal outcomes. In contrast, the county-level longitudinal associations between SDOH

and stroke mortality in our case are unobservable. For clustering of these associations, one might consider applying the finite mixture of regression models (Jacobs et al., 1991; Jiang and Tanner, 1999) to the SDOH and stroke mortality longitudinal data. However, this method cannot capture longitudinal changes in the associations within the clustering procedures, potentially resulting in unreliable clustering outcomes due to the disregard of longitudinal signals. In light of functional data analysis (Ramsay and Silverman, 2002, 2005), some studies proposed a finite mixture of functional regression models for clustering longitudinal associations (Yao et al., 2011; Lu and Song, 2012). Nonetheless, they do not address the issue of collinearity among covariates in their functional regression models. In our study, the collection of SDOH serves as functional covariates and exhibits significant collinearity, stemming from their derivation from multiple domains (e.g., social, economic, and environmental domains). In this case, ignoring colinearity among the SDOH data may lead to misspecification in the functional regression model. This oversight could compromise the accuracy of the resultant clustering outcome.

Furthermore, to enhance interpretability, existing studies analyzing associations between SDOH and stroke mortality often adopt a pre-selection step on the SDOH covariates (Tsao et al., 2022, 2023), as their number is usually large, containing hundreds of variables. In our case, the pre-selection of longitudinal SDOH data can be achieved through variable selection in functional regression models (Wang et al., 2008; Kong et al., 2016; Goldsmith and Schwartz, 2017). However, these methods generally assume that associations between covariates and responses are invariant across different samples. This assumption limits their direct applicability to our case, where SDOH covariates may exhibit distinct associations with stroke mortality among different counties. Moreover, performing selections of SDOH prior to clustering may introduce biases for the subsequent clustering outcome, as

the selection of SDOH is unrelated to the clustering process. On the other hand, without proper selection of SDOH, the clustering process may be statistically inefficient due to the complex structure of longitudinal SDOH data, which possess high-dimensionality and functional nature simultaneously. To accommodate such a complicated structure, it would be beneficial to connect variable selections of SDOH to the clustering of longitudinal associations, yet this topic is rarely discussed in the literature.

In this article, we introduce a novel method for simultaneous clustering and variable selection of longitudinal associations between SDOH and stroke mortality in US counties. Our method, based on a finite mixture of functional linear concurrent models (FMFLCM), incorporates a new class of smoothness-sparsity pursued penalties to address the functional nature and high-dimensionality of the SDOH data. These penalties are designed to borrow information from distinct clusters of the FMFLCM, thereby enhancing statistical efficiency for both clustering and variable selection, and simultaneously addressing the collinearity issue among the SDOH data. For the estimation, we develop a novel regularized expectation-maximization (REM) algorithm by incorporating the proposed penalties. This approach allows for the clustering of longitudinal associations while embedding a variable selection step of SDOH covariates. As a result, the cluster memberships and the selected SDOH can be iteratively updated within the REM algorithm. This iterative updating process helps mitigate potential biases stemming from the selected covariates during the clustering process. Through these procedures, we provide a novel data-driven method for county-level regional division, aiming to offer insights into region-specific stroke prevention measures for US counties.

The remainder of this article is organized as follows. In Section 2, we begin by introducing the SDOH and stroke mortality dataset, and then proceed to demonstrate some of

their data features in Section 2.1. Following this, we present the FMFLCM in Section 2.2, followed by the demonstration of sparsity and smoothness pursued penalties in Section 2.3, and the REM in Section 2.4. In Section 3, we conduct simulation studies to compare the proposed methods with some competing approaches in terms of clustering performance, variable selection, and parameter estimation. In Section 4, we apply the proposed clustering method to our dataset and present the clustering result, along with the estimation relating to the selected SDOH. Finally, We provide conclusions and discussion in Section 5.

2 Methodologies

2.1 Data Source

In 2020, the Agency for Healthcare Research and Quality (AHRQ) compiled and released a SDOH database for a better understanding of community-level factors, healthcare quality and delivery, and individual health. The SDOH database contains yearly records of 345 SDOH collected from 3226 counties from 2009 to 2018. These SDOH are classified into 5 domains: (1) social context, such as age, race and ethnicity, and veteran status; (2) economic context, such as income and unemployment; (3) education; (4) physical infrastructure, such as housing, food insecurity, and transportation; and (5) health care contexts, such as health insurance coverage and health care access. To study the association between the SDOH and stroke mortality, we connect the SDOH database with a stroke mortality data provided by the Interactive Atlas of Heart Disease and Stroke at the Centers for Disease Control and Prevention (CDC) on the county level. The stroke mortality database was originally compiled from 2 data sources: (1) the National Vital

Statistics System at the National Center for Health Statistics, and (2) the hospital discharge data from the Centers for Medicare & Medicaid Services' Medicare Provider Analysis and Review (MEDPAR) file. All data and materials used in this analysis are publicly available at the AHRQ website: <https://www.ahrq.gov/sdoh/index.html> and CDC website <https://www.cdc.gov/dhdsp/maps/atlas/index.htm>. Since the AHRQ database is HIPAA (Health Insurance Portability and Accountability Act) compliant, our data do not require to be reviewed by an institutional review board.

It's worth noting that the SDOH dataset contains missing values. Following the approach of a previous study on the dataset (Son et al., 2023), we exclude the SDOH variables that have a missing proportion of more than 60%. The average missing proportion of the remaining variables is 3.6%. For these missing values, we employ a k-nearest neighbors (KNN) method (Kowarik and Templ, 2016) to impute the SDOH data, ensuring the SDOH and stroke mortality data are aligned with time for each county. The detailed implementation of the KNN is provided in Part A of the Supplementary Material.

As mentioned previously, significant collinearity may exist among the SDOH data. This phenomenon is observed in our dataset, where the longitudinal data between some of the SDOH exhibit significant correlations as illustrated in Figure 1. Besides, coinciding with the previous studies (Villablanca et al., 2016; He et al., 2021; Son et al., 2023), evident regional disparities and longitudinal variations can also be observed in the SDOH – stroke mortality associations from our dataset. To demonstrate this, we calculate the yearly Pearson correlation between stroke mortality and the percentage of Asian and Pacific Island language speakers (PAPL), one principal sociocultural factor in the SDOH. To calculate the yearly correlations, we first divide the counties in the US into several regions, and presume that the counties in a divided region exhibit the same SDOH – stroke mortality

correlation. We consider two types of divisions: state-wise division (Zelko et al., 2023) and rural-urban division (Son et al., 2023). The yearly correlations from 2009-2018 for each state, or for rural and urban areas, are presented in panels (B) and (D) of Figure 2, respectively. Besides, we also present the geographical maps of correlations for the years 2009, 2013, and 2018 in panels (A) and (C) of Figure 2, respectively for two types of division strategies.

From the maps in Figure 2, we observe significant regional disparities in the correlations among different states, as well as between rural and urban areas. These correlations all exhibit changes over time. In addition, we find that the longitudinal correlations in rural and urban areas (shown in panel (D) of Figure 2) are consistently negative over time, while the correlations from some states (such as Nevada, as seen in panel (B) of Figure 2) are mostly positive. These results suggest that the outcomes of longitudinal associations are highly sensitive to the region division strategy, and different region divisions may lead to inconsistent conclusions for the stroke management. As such, we require a reasonable data-driven method for the region division in exploring SDOH – stroke mortality associations.

2.2 Finite Mixture of Functional Linear Concurrent models

Let $Y_i(t) \in \mathbb{R}$ and $\mathbf{X}_i(t) := (X_{i1}(t), \dots, X_{ip}(t))^T \in \mathbb{R}^p$ represent the stroke mortality and SDOH data in the i th county at time t , respectively, where $i = 1, \dots, n$ and $t \in \mathcal{T}$, with n being the number of counties and \mathcal{T} being the observed time period. Here, $Y_i(\cdot)$ and $\mathbf{X}_i(\cdot)$ are considered the functional response and covariate samples, respectively, with n and p being the sample size and dimension of the covariates. Without loss of generality, \mathcal{T} is $[0, 1]$ in this article.

We focus on the association between $Y_i(t)$ and $\mathbf{X}_{i(t)}$ for $t \in [0, 1]$, referred to as lon-

gitudinal associations in what follows. To cluster the longitudinal associations of different counties i , we assume the samples $\{Y_i(\cdot), \mathbf{X}_i(\cdot); i = 1, \dots, n\}$ can be divided into K clusters and follow a finite mixture of functional linear concurrent models

$$Y_i(t) = \sum_{j=1}^p X_{ij}(t)\beta_{jk}(t) + \varepsilon_{ik}(t) \text{ if } Z_i = k, \quad (1)$$

where Z_i is the cluster membership for the i th subject, $\beta_{jk}(\cdot)$ is the functional coefficient for the k th group to capture the longitudinal associations between the response and the j th covariate, and $\varepsilon_{ik}(t)$ is a Gaussian white noise with variance σ_k^2 for each k . We assume that the white noise processes $\{\varepsilon_{ik}(\cdot); i = 1, \dots, n, k = 1, \dots, K\}$ are independent across different i s and k s, and Z_1, \dots, Z_n are i.i.d. samples from a multinomial distribution on $\{1, \dots, K\}$ with $\mathbb{P}(Z_i = k) = \pi_k$.

Let $\boldsymbol{\beta}(t) = \{\beta_{jk}(t)\}_{j=1, \dots, p; k=1, \dots, K}$, $\boldsymbol{\sigma}^2 := (\sigma_1^2, \dots, \sigma_K^2)^T$ and $\boldsymbol{\pi} := (\pi_1, \dots, \pi_K)^T$. We use $\boldsymbol{\beta}_{\cdot k}(t)$ and $\boldsymbol{\beta}_{j \cdot}(t)$ to denote the k th column and the j th row of $\boldsymbol{\beta}(t)$, respectively. For ease of notation, we might use $\boldsymbol{\beta}$, $\boldsymbol{\beta}_{\cdot k}$, $\boldsymbol{\beta}_{j \cdot}$, and β_{jk} to represent $\boldsymbol{\beta}(\cdot)$, $\boldsymbol{\beta}_{\cdot k}(\cdot)$, $\boldsymbol{\beta}_{j \cdot}(\cdot)$ and $\beta_{jk}(\cdot)$ in what follows.

Since our dataset are only observed on a finite time grid, we assume that $\{(Y_i(t_{is}), \mathbf{X}_i(t_{is})); i = 1, \dots, n, s = 1, \dots, S_i\}$ is the observed data for FMFLCM, where $\{t_{is}; i = 1, \dots, n, s = 1, \dots, S_i\} \subset \mathcal{T}$. The log-likelihood of the parameters $\boldsymbol{\Phi} := (\boldsymbol{\beta}, \boldsymbol{\sigma}^2, \boldsymbol{\pi})$ is then given as

$$l(\boldsymbol{\Phi}) = \sum_{i=1}^n \sum_{s=1}^{S_i} \log \left\{ \sum_{k=1}^K \pi_k f(Y_i(t_{is}); \mathbf{X}_i(t_{is})^T \boldsymbol{\beta}_{\cdot k}(t_{is}), \sigma_k^2) \right\}, \quad (2)$$

where $f(\cdot; \mu, \sigma^2)$ is a Gaussian density function with mean μ and variance σ^2 . One may adopt the maximum likelihood estimator (MLE) of (2) to estimate $\boldsymbol{\Phi}$. However, given that the functional coefficient $\boldsymbol{\beta}$ is an infinite-dimensional parameter, the optimization of $\boldsymbol{\beta}$ in

(2) is generally an ill-posed problem. Furthermore, the MLE of β may also suffer from the curse of dimensionality, i.e., p is large. For this case, the MLE of (2) may be far from its true value, or even does not exist (Wang et al., 2008; Yi and Caramanis, 2015).

To solve the above issues, we propose a class of penalties in Section 2.3 to regularize the smoothness and the sparsity of β . Based on the proposed penalties, we develop a regularized expectation maximization algorithm in Section 2.4 to implement the clustering for subjects, the estimation for β , and the variable selections for the covariates simultaneously.

2.3 Sparsity and Smoothness Pursued Penalties

In this subsection, we propose a class of smoothly clipped absolute deviation (SCAD) type penalties (Fan and Li, 2001) to adjust the aforementioned ill-posed problems. The SCAD penalty takes the form

$$P_{\text{SCAD}}(u; \lambda) = \begin{cases} \lambda u & \text{if } 0 \leq u \leq \lambda, \\ -\frac{(u^2 - 2\gamma\lambda u + \lambda^2)}{2(\gamma-1)} & \text{if } \lambda < u < \gamma\lambda, \\ \frac{(\gamma+1)\lambda^2}{2} & \text{if } u \geq \gamma\lambda, \end{cases}$$

where u is a scalar parameter to be penalized, λ is a tuning parameter, and γ is a hyperparameter chosen to be 3.7 as suggested in Fan and Li (2001). We extend the SCAD penalty for the functional objects β , which is the functional SCAD (FSCAD) penalty

$$P_{\text{FSCAD}}(\beta; \lambda, r) := \sum_{j=1}^p \sum_{k=1}^K P_{\text{SCAD}}(\|\beta_{jk}\|_r; \lambda), \quad (3)$$

where $\|\beta_{jk}\|_r = \sqrt{\|\beta_{jk}\|^2 + r\|\beta_{jk}''\|}$ with $\|f\| = \sqrt{\int f^2(t) dt}$ being an L_2 norm for a function f . Here, $\|\beta_{jk}\|_r$ measures the magnitude and smoothness of β_{jk} simultaneously (Meier et al., 2009), in which r leverages the function’s magnitude and smoothness in the norm. By penalizing β using (3), we can penalize the smoothness of each β_{jk} to deal with its functional nature, and shrink the β_{jk} with small norm $\|\beta_{jk}\|_r$ to zero (Huang et al., 2009) for the purpose of variable selections.

It’s worth noting that our SDOH functional covariates exhibit significant collinearity as illustrated in Figure 1, and the presence of the collinearity may enlarge variance and lead to misspecification in variable selections (Zou and Hastie, 2005). To adjust for this issue, we adopt a similar strategy as the elastic net (Zou and Hastie, 2005) to add an L_2 term to the FSCAD penalty (3). As such, we obtain the functional SCAD-Net (FSCAD-Net) penalty

$$\mathbf{P}_{\text{FSCAD-Net}}(\beta; \lambda, \rho, r) := \sum_{j=1}^p \sum_{k=1}^K \left\{ \rho \mathbf{P}_{\text{FSCAD}}(\beta_{jk}; \lambda, r) + (1 - \rho) \lambda_k \|\beta_{jk}\|_r^2 \right\}, \quad (4)$$

where $\rho \in [0, 1]$ is a tuning parameter controlling the proportions between the FSCAD and L_2 terms. The above penalty maintains the properties of the FSCAD penalty. In addition, the FSCAD-Net penalty can reduce variance and address misspecification in variable selections by penalizing the magnitude of $\sum_{j=1}^p \sum_{k=1}^K \|\beta_{jk}\|_r^2$.

It’s worth noting that the variable selections with FSCAD or FSCAD-Net do not guarantee that the selected covariates from different clusters are the same. This may not be reasonable for some applications, in which we need to identify the important variables for all clusters. In our case, the purpose of variable selections for SDOH is to facilitate the clustering on the selected SDOH covariates. To this end, we require the selected SDOH for all clusters to be the same within the estimation procedure. To facilitate such kind of

investigation, we propose to shrink $\{\beta_{jk}; k = 1, \dots, K\}$ to zero functions simultaneously within the variable selection, which is referred to as cluster-invariant sparsity. For this, we modify the FSCAD-Net penalty into the functional group SCAD-Net (FGSCAD-Net) penalty

$$\mathbf{P}_{\text{FGSCAD-Net}}(\boldsymbol{\beta}; \lambda, \rho, r) := \sum_{j=1}^p \left\{ \rho \mathbf{P}_{\text{SCAD}}(\|\boldsymbol{\beta}_j\|_r; \lambda) + (1 - \rho)\lambda \|\boldsymbol{\beta}_j\|_r^2 \right\}, \quad (5)$$

where $\|\boldsymbol{\beta}_j\|_r = \sqrt{\sum_{k=1}^K \|\beta_{jk}\|_r^2}$. By grouping $\{\beta_{kj}; k = 1, \dots, K\}$ for each j together in the norm, the FGSCAD-Net not only yields cluster-invariant sparsity but also improves statistical efficiency for variable selection by borrowing strength from all clusters for estimating $\boldsymbol{\beta}$.

2.4 Regularized EM Algorithm

In this subsection, we apply an EM algorithm to conduct the parameter estimation of FMFLCM. We first introduce a latent variable $z_{ik} := I(Z_i = k)$ to represent the cluster membership of the subject i , where $I(\cdot)$ is an indicator function. Denote \mathbf{Z} as $\{z_{ik}; i = 1, \dots, n, k = 1, \dots, K\}$. The complete log-likelihood of FMFLCM containing \mathbf{Z} is then given by

$$l_C(\boldsymbol{\Phi}, \mathbf{Z}) = \sum_{i=1}^n \sum_{k=1}^K z_{ik} \sum_{s=1}^{S_i} \left[\log \pi_k + \log \left\{ f(Y_i(t_{is}); \{\mathbf{X}_i(t_{is})\}^T \boldsymbol{\beta}_{\cdot k}(t_{is}), \sigma_k^2) \right\} \right]. \quad (6)$$

In order to solve the ill-posed issue for estimating $\boldsymbol{\beta}$, we employ a regularized EM (REM) algorithm using the FGSCAD-Net penalty (5) as proposed in Section 2.3. In the following, we demonstrate the E-step and M-step of the REM algorithm.

2.4.1 General procedures of REM algorithm

Let $\Phi^{(m-1)} := (\boldsymbol{\beta}^{(m-1)}, (\boldsymbol{\sigma}^2)^{(m-1)}, \boldsymbol{\pi}^{(m-1)})$ be the parameters updated at the $(m-1)$ th iteration.

E-step: With the parameter $\Phi^{(m-1)}$, we first compute the conditional expectation of z_{ik} given the samples $\mathbf{Y} = \{Y_i(t_{is}); i = 1, \dots, n, s = 1, \dots, S_i\}$ and $\mathbf{X} = \{\mathbf{X}_i(t_{is}); i = 1, \dots, n, s = 1, \dots, S_i\}$

$$\omega_{ik}^{(m)} := \mathbb{E}_{\Phi^{(m-1)}}(z_{ik} \mid \mathbf{Y}, \mathbf{X}) = \frac{\pi_k^{(m-1)} \sum_{s=1}^{S_i} f\left(Y_i(t_{is}), \mathbf{X}_i(t_{is})^T \boldsymbol{\beta}_{\cdot k}^{(m-1)}(t_{is}), (\sigma_k^2)^{(m-1)}\right)}{\sum_{k=1}^K \pi_k^{(m-1)} \sum_{s=1}^{S_i} f\left(Y_i(t_{is}), \mathbf{X}_i(t_{is})^T \boldsymbol{\beta}_{\cdot k}^{(m-1)}(t_{is}), (\sigma_k^2)^{(m-1)}\right)}. \quad (7)$$

After that, we calculate the expectation of the complete log-likelihood in (6) conditioning on \mathbf{Y} and \mathbf{X} , given the parameter $\Phi^{(m-1)}$. This leads to the Q function

$$Q(\Phi \mid \Phi^{(m-1)}) := \sum_{i=1}^n \sum_{k=1}^K \omega_{ik}^{(m)} \sum_{s=1}^{S_i} \left[\log \pi_k + \log \left\{ f\left(Y_i(t_{is}), \{\mathbf{X}_i(t_{is})\}^T \boldsymbol{\beta}_{\cdot k}(t_{is}), \sigma_k^2\right) \right\} \right]. \quad (8)$$

M-step: To facilitate the update of $\boldsymbol{\beta}$, we incorporate the FGSCAD-Net penalty (5) into the Q function (8).

$$Q^{\text{pen}}(\Phi \mid \Phi^{(m-1)}; \lambda, \rho, r) := Q(\Phi \mid \Phi^{(m-1)}) - \mathbf{P}_{\text{FGSCAD-Net}}(\boldsymbol{\beta}; \lambda, \rho, r). \quad (9)$$

According to (9), we separately update the parameters $\boldsymbol{\beta}$, $\boldsymbol{\sigma}^2$, and $\boldsymbol{\pi}$, given the current tuning parameters λ, ρ, r . In detail, holding $\boldsymbol{\sigma}^2$ and $\boldsymbol{\pi}$ fixed at their previous values at the $(m-1)$ th iteration, we update $\boldsymbol{\beta}$ as

$$\boldsymbol{\beta}^{(m)} = \operatorname{argmax}_{\boldsymbol{\beta}} Q^{\text{pen}}\left(\left(\boldsymbol{\beta}, (\boldsymbol{\sigma}^2)^{(m-1)}, \boldsymbol{\pi}^{(m-1)}\right) \mid \Phi^{(m-1)}; \lambda, \rho, r\right). \quad (10)$$

Once obtaining $\boldsymbol{\beta}^{(m)}$, we update $\boldsymbol{\pi}^{(m)}$ by

$$\pi_k^{(m)} = \frac{\sum_{n=1}^N \omega_{ik}^{(m)}}{N}, \quad k = 1, \dots, K, \quad (11)$$

and update $(\boldsymbol{\sigma}^2)^{(m)}$ by

$$(\sigma_k^2)^{(m)} = \frac{\sum_{i=1}^N \omega_{ik}^{(m)} \sum_{s=1}^{S_i} \left\{ Y_i(t_{is}) - \mathbf{X}_i(t_{is})^T \boldsymbol{\beta}_k^{(m)}(t_{is}) \right\}^2}{\sum_{i=1}^N S_i \omega_{ik}^{(m)}}, \quad k = 1, \dots, K, \quad (12)$$

where $\omega_{ik}^{(m)}$ is defined in (7). Note that the main efforts for the above procedures lie in the optimization in (10). We demonstrate this process in detail in Sections 2.4.2.

2.4.2 Optimization of FGSCAD-Net Regularization

For the functional parameter $\boldsymbol{\beta}(t)$, we parameterize its (j, k) th element, which is $\beta_{jk}(t)$, by the cubic spline basis functions $\psi_1(t), \dots, \psi_L(t)$ with equally spaced knots on \mathcal{T} . We assume that

$$\beta_{jk}(t) = \mathbf{b}_{jk}^T \boldsymbol{\Psi}(t), \quad (13)$$

where $\mathbf{b}_{jk} = (b_{jk1}, \dots, b_{jkL})^T$ and $\boldsymbol{\Psi}(t) = (\psi_1(t), \dots, \psi_L(t))^T$. We then maximize (10) by substituting (13) into (9). We use $\mathbf{Q}^T \mathbf{Q}$ to denote the Cholesky decomposition of the non-negative definite matrix

$$\int_{\mathcal{T}} \boldsymbol{\Psi}(t) \{\boldsymbol{\Psi}(t)\}^T + r \boldsymbol{\Psi}''(t) \{\boldsymbol{\Psi}''(t)\}^T dt,$$

where \mathbf{Q} is an upper triangular matrix. With this, we define $\boldsymbol{\alpha}_{j\cdot} = (\boldsymbol{\alpha}_{j1}^T, \dots, \boldsymbol{\alpha}_{jk}^T)^T$ with $\boldsymbol{\alpha}_{jk} = \mathbf{Q}\mathbf{b}_{jk}$ and rewrite $\|\boldsymbol{\beta}_{j\cdot}\|_r$ as

$$\begin{aligned}\|\boldsymbol{\beta}_{j\cdot}\|_r &= \sqrt{\|\boldsymbol{\beta}_{j\cdot}\|^2 + r\|(\boldsymbol{\beta}_{j\cdot})''\|^2} \\ &= \sqrt{\sum_{k=1}^K \int \mathbf{b}_{jk}^T \boldsymbol{\Psi}(t) \{\boldsymbol{\Psi}(t)\}^T \mathbf{b}_{jk} + r \mathbf{b}_{jk}^T \boldsymbol{\Psi}''(t) \{\boldsymbol{\Psi}''(t)\}^T \mathbf{b}_{jk} dt} \\ &= \sqrt{\sum_{k=1}^K (\mathbf{Q}\mathbf{b}_{jk})^T \mathbf{Q}\mathbf{b}_{jk}} = \|\boldsymbol{\alpha}_{j\cdot}\|,\end{aligned}$$

where we abuse the notation $\|\cdot\|$ to denote the Euclidean norm of a vector. We further denote $\boldsymbol{\alpha}_{\cdot k} = (\boldsymbol{\alpha}_{1k}^T, \dots, \boldsymbol{\alpha}_{pk}^T)^T$, $h_{ij}(t) = (X_{ij}(t)\psi_1(t), \dots, X_{ij}(t)\psi_L(t))^T \mathbf{Q}^{-1}$ and $\mathbf{H}_i(t) = (h_{i1}(t), \dots, h_{ip}(t))^T$. Then we can transform the optimization (10) into the standard group SCAD- L_2 optimization problem (Zeng and Xie, 2014) as follows

$$(\tilde{\boldsymbol{\alpha}}_{\cdot 1}^{(m)}, \dots, \tilde{\boldsymbol{\alpha}}_{\cdot K}^{(m)}) = \operatorname{argmax}_{\boldsymbol{\alpha}_{\cdot 1}, \dots, \boldsymbol{\alpha}_{\cdot K}} Q(\boldsymbol{\Phi} \mid \boldsymbol{\Phi}^{(m-1)}) - \sum_{j=1}^p \{P_{\text{SCAD}}(\|\boldsymbol{\alpha}_{j\cdot}\|; \lambda) + \rho \|\boldsymbol{\alpha}_{j\cdot}\|^2\}, \quad (14)$$

where $Q(\boldsymbol{\Phi} \mid \boldsymbol{\Phi}^{(m-1)})$ can be expressed in terms of $\{\boldsymbol{\alpha}_{\cdot k}; k = 1, \dots, K\}$ by

$$Q(\boldsymbol{\Phi} \mid \boldsymbol{\Phi}^{(m-1)}) = \sum_{i=1}^n \sum_{k=1}^K \omega_{ik}^{(m)} \sum_{s=1}^{S_i} \left[\log \pi_k^{(m-1)} + \log \left\{ f(Y_i(t_{is}), \{\mathbf{H}_i(t_{is})\}^T \boldsymbol{\alpha}_{\cdot k}, (\sigma_k^2)^{(m-1)}) \right\} \right].$$

This optimization problem can be efficiently solved by the group coordinate descent algorithm (Breheny and Huang, 2015).

Since the estimators involved with L_2 terms are generally biased (Zou and Zhang, 2009; Zeng and Xie, 2014), we conduct a bias correction for $\tilde{\boldsymbol{\alpha}}_{\cdot k}^{(m)}$. In detail, we use the following

bias correction formula to obtain the final estimation of $\boldsymbol{\alpha}_{\cdot k}^{(m)}$ (Zeng and Xie, 2014)

$$\boldsymbol{\alpha}_{\cdot k}^{(m)} = \{1 + 2(1 - \rho)\lambda\} \tilde{\boldsymbol{\alpha}}_{\cdot k}^{(m)}. \quad (15)$$

Once obtaining $\boldsymbol{\alpha}_{\cdot k}^{(m)}$, we compute $\boldsymbol{\beta}_{\cdot k}^{(m)}(t)$ by

$$\boldsymbol{\beta}_{\cdot k}^{(m)}(t) = \mathbf{Q}^{-1} \boldsymbol{\alpha}_{\cdot k}^{(m)} \boldsymbol{\Psi}(t). \quad (16)$$

2.4.3 Tuning Strategy

The REM algorithm requires tuning of three hyperparameters λ , ρ , and r . The traditional strategy for choosing λ , ρ , and r needs to run the entire algorithm for all candidate combinations of (λ, ρ, r) . This is computationally inefficient since there are numerous choices of candidate combinations that need to be examined. Inspired by the path-fitting algorithm (Breheeny and Huang, 2015) for a fast tuning of λ , we modify the traditional tuning strategy for the REM algorithm. Instead of running a complete REM for each candidate of λ , we propose to tune λ in each M-step of the REM algorithm; refer Part B.2 in Supplementary Material for the implementation details. By this approach, we can employ a path-fitting algorithm to select λ for accelerating the tuning process (Huang et al., 2009; Li et al., 2016; Cai et al., 2019).

For the hyperparameters ρ and r , we run an entire REM for each of their candidate combinations, nested with the aforementioned strategy for tuning λ . We select ρ and r from the optional values based on the AIC

$$\text{AIC}(\rho, r) = -2l(\hat{\boldsymbol{\Phi}}) + 2\text{df}, \quad (17)$$

where $\widehat{\Phi}$ is the converged parameters of the REM algorithm given the current choices of ρ and r , and df is the degree of freedom determined as in Breheny and Huang (2015).

In addition, we need to provide the group number K for the implementation of the REM algorithm. To determine K , we similarly treat it as a tuning parameter, and proceed with its selection by minimizing the BIC

$$\text{BIC}(K) = -2l(\Phi_K) + \text{df}(\lambda) \cdot \log\left(\sum_{i=1}^n S_i\right), \quad (18)$$

where Φ_K is the converged parameters when the number of clusters is K , with ρ and r selected based on (17). The complete REM algorithm with the tuning processes are summarized in Algorithm 1 in Part B.1 of Supplementary Material.

3 Simulation

In this section, we conduct numerical simulations to assess the performances of the proposed method in Section 2, in comparison to other competing methods across three aspects: clustering, variable selection, and parameter estimation. To begin with, we generate the functional covariates $\mathbf{X}_i(\cdot)$, $i = 1, \dots, n$, as

$$\mathbf{X}_i(t) = \sum_{l=1}^4 \boldsymbol{\theta}_{il} \psi_l(t), \quad \forall t \in [0, 1],$$

where $\psi_1(\cdot), \dots, \psi_4(\cdot)$ are the first four nonconstant Fourier basis functions, and $\boldsymbol{\theta}_{il} \in \mathbb{R}^p$, for each i and l , is a random vector sampled from a mean-zero Gaussian distribution with the covariance matrix $\{l^{-2}\alpha^{|j-k|}\}_{1 \leq j, k \leq p} \in \mathbb{R}^{p \times p}$. Here, the parameter α controls the dependence between covariates, with a higher value indicating stronger dependencies.

To generate the functional coefficients attaining the cluster-invariant sparsity, we set

$\boldsymbol{\beta}_k(t) \in \mathbb{R}^p$ as

$$\boldsymbol{\beta}_k(t) = (f_{1k}(t), f_{1k}(t), f_{2k}(t), f_{2k}(t), f_{3k}(t), f_{3k}(t), 0, \dots, 0)^T, \quad k = 1, \dots, K, \quad t \in [0, 1],$$

where $f_{jk}(t) = f_{jk}^*(t) / \|f_{jk}^*\|_2$, and $f_{jk}^*(\cdot)$ s are given by

$$\begin{aligned} f_{11}^*(t) &= \sin\left(\frac{\pi t}{2} + \frac{3}{2}\pi\right) - t - \frac{1}{2}, & f_{12}^*(t) &= \{\cos(2\pi t) - 1\}^2, & f_{13}^*(t) &= -f_{11}^*(t) + 1, \\ f_{21}^*(t) &= \sin(2\pi t) - t + 0.5, & f_{22}^*(t) &= \sin\left(\frac{\pi t}{2} + \pi\right), & f_{23}^*(t) &= -f_{21}^*(t) - 0.5, \\ f_{31}^*(t) &= -\sin\left(\frac{\pi t}{2} + \frac{3\pi}{2}\right) - t - 0.5, & f_{32}^*(t) &= -f_{12}^*(t), & f_{33}^*(t) &= f_{11}^*(t) + t + 0.5. \end{aligned}$$

These functions are presented in Figure 2 in Supplementary Material. Note that the relevant covariates for all clusters are X_{i1}, \dots, X_{i6} , each of which makes an equal contribution to Y_i since $\|f_{jk}\|_2 = 1$ for $j = 1, \dots, 6$ and $k = 1, \dots, K$. We set $K = 3$.

Next, we generate the cluster membership Z_i from a multinomial distribution as described in Section 2, with $\pi_k = 1/K$, $k = 1, \dots, K$. Providing $\mathbf{X}_i(t)$, Z_i , and $\boldsymbol{\beta}(t)$, $Y_i(t)$ is generated from the model (1) for t contained in 10 equally spaced knots on $[0, 1]$, where the variance of the error term σ_k^2 is taken according to the signal-to-noise ratio (SNR)

$$\sigma_k^2 = \left\{ \frac{\sum_{i=1}^n \int_{\mathcal{T}} \sum_{k=1}^K I(Z_i = k) \{\mathbf{X}_i(t)^T \boldsymbol{\beta}_k(t)\}^2 dt}{n} \right\} / \text{SNR}.$$

We set the SNR as 12. Based on this setting, we evaluate the method proposed in Section 2, which is abbreviated as FGS-Net due to the use of FGSCAD-Net penalty (5). We compare FGS-Net by other REM methods penalized with the FSCAD-Net penalty (4), and FSCAD penalty (3), abbreviated as FS-Net and FS in the following. Apart from these three methods, we examine other competing methods for clustering longitudinal associations.

- RP: This method incorporates a roughness penalty (RP) into the REM algorithm, which is given as $\sum_{j=1}^p \sum_{k=1}^K \lambda \|\beta_{jk}''\|_2^2$.
- VS-RP: This method first utilizes the FGS-Net with $K = 1$ to conduct the variable selection (VS), where the clustering is not performed at this stage. After that, we adopt the selected variables to implement the RP method for clustering.
- LI-MIX: This method fits the data by a finite mixture of linear regression models (LI-MIX), i.e., the functional coefficient $\beta_{jk}(t)$ in (1) is treated as a constant over t . To perform this method, we first conduct a variable selection using ordinary linear regression models shrunk with an elastic-net penalty (Zou and Zhang, 2009). After that, we adopt the selected covariates to fit a finite mixture of linear regression models for the clustering (Khalili and Chen, 2007).

The RP is a simplification of the FS-Net with $\rho = 0$, which only regularizes the roughness of each β_{jk} and does not yield sparsity. VS-RP and LI-MIX are two two-step approaches, which implement the variable selection and clustering orderly. These two-step methods are more simple than the aforementioned FGS-Net, FS-Net, FS, and RP. However, selecting relevant covariates prior to the clustering procedure may raise additional problems, as the clustering performance may be sensitive to the outcome from the variable selection. It's worth noting that LI-MIX further ignores the time-varying nature of β_{jk} .

For each scenario with different combinations of n , p , and α , the simulations are repeated 100 times. We adopt random initialization for the FGS-Net, FS-Net, and FS methods, i.e., set $\omega_{ik}^{(0)} = I(Z_i^{(0)} = k)$, where $Z_i^{(0)}$ is sampled from a multinomial distribution as described in Section 2, with $\pi_k = 1/K$, $k = 1, \dots, K$. On the other hand, RP, VS-RP, and LI-MIX are initialized with the actual cluster membership $\omega_{ik}^{(0)} = I(Z_i = k)$. To alleviate computation burdens, we only use one initialization for each simulation. Moreover, the K in RP, VS-RP,

and LI-MIX is fixed to 3, the true number of clusters. The K for FGS-Net, FS-Net, and FS are selected based on (18) in Section 2.4.3.

The performance of clustering, variable selection, and parameter estimation is evaluated based on the following criteria.

- Clustering accuracy is evaluated using the adjusted Rand Index (ARI, Rand, 1971).

The ARI is bounded by ± 1 to measures the similarity between the true cluster membership and the estimated cluster membership. A higher ARI represents a better clustering result.

- Variable selection performance is evaluated using C and IC, where C is the number of zero coefficients that are correctly estimated to zero

$$C = \sum_{j=7}^p \sum_{k=1}^K I(\|\hat{\beta}_{jk}\|_2 = 0),$$

where $\hat{\beta}_{jk}$ is the estimate of β_{jk} . Similarly, IC is the number of nonzero coefficients that are incorrectly estimated to zero

$$IC = \sum_{j=1}^6 \sum_{k=1}^K I(\|\hat{\beta}_{jk}\|_2 = 0).$$

- The parameter estimation accuracy is measured using the standardized mean square error (MSE) of the functional coefficients, which is defined as

$$MSE = \frac{\sum_{k=1}^K \sum_{j=1}^p \|\beta_{jk} - \hat{\beta}_{jk}\|_2^2}{\sum_{k=1}^K \sum_{j=1}^p \|\beta_{jk}\|_2^2}.$$

We investigate performances of the above methods under various scenarios of n , p , and α . Here, we set n to 180 or 300, and take p as 10, $n/6$, $n/2$, and $3n/4$, to consider the

situations ranging from a small to a large number of covariates. Additionally, we set α to 0.4 and 0.8 to reflect the mild or strong dependence among the covariates. The averaged ARI, C, IC, and MSE are presented in Table 1. In the analysis below, we only focus on the results of $n = 180$. Similar conclusions can be obtained from the result of $n = 300$.

Overall, FGS-Net, FS-Net, and FS show superior performance under different scenarios of n , p , and α , highlighting the advantages of implementing variable selection and clustering simultaneously under the REM framework. In contrast, the RP method only uses a roughness penalty and does not consider variable selections within the clustering. As a result, its performance quickly deteriorates for both clustering and parameter estimation as p increases. Furthermore, among the two-step methods, we find that the VS-RP performs poorly compared to the first three REM-type methods. For instance, in all scenarios with $n = 180$, the average ICs of VS-RP are mostly larger than 9, indicating that about half of the nonzero functional coefficients are incorrectly identified as zero. This leads to significant estimation errors in both clustering and parameter estimation by the VS-RP method, and suggests that selecting variables before clustering is ineffective. It's worth noting that the results of LI-MIX are even worse, as this method further ignores the time-varying nature of $\beta(\cdot)$ in the estimation procedure.

In Table 1, we also observe that the ICs and MSEs of FS are significantly larger than those of FS-Net as α increases. This is expected since the dependencies between functional covariates may impede the performance of the FS procedure. This requires an additional ridge-type penalty in the FS-net to stabilize the estimation procedure. Moreover, as p increases, the ICs and MSEs of FS-Net are further larger than those of FGS-net. For these cases, the high-dimensionality would undermine the statistical efficiency for both variable selection and clustering in the FS-Net. Therefore, it would be beneficial to impose

cluster-invariant sparsity through FGS-net to borrow strengths across all clusters.

In the case of $n = 180$, $p = 240$, and $\alpha = 0.8$, we further illustrate the estimation performance of the functional coefficients in Figure 3. We observe that the estimations of FS-Net exhibit smaller biases compared to FS, highlighting the significance of FS-Net in mitigating biases of functional coefficients. Furthermore, in comparison to those of FS-Net and FS, the estimated curves of FGS-Net show even smaller biases and narrower confidence bands, owing to the pursuit of cluster-invariant sparsity. Overall, FGS-Net is the most suitable choice among these six methods for clustering longitudinal associations and selecting important variables in high-dimensional functional covariates.

4 Real data

In this section, we apply our method to the SDOH and stroke mortality dataset for the clustering of their longitudinal associations. Given that the stroke mortality data are right-skewed and take positive values, we conduct a log transformation to stabilize its variance. Using our approach, we identify 2 clusters for the longitudinal associations and 18 relevant SDOH covariates for stroke mortality.

The two clusters for the county-level longitudinal associations are presented in Figure 4. The proportions of two clusters, determined by the number of counties, stand at 68% and 32%, respectively. Notably, both clusters are prevalent across the majority of states in the US, encompassing both rural and urban areas (urban: 76% and 24%, and rural: 65% and 35%, for cluster 1 and cluster 2, respectively). It's worth noting that the southeastern US contains a region called the Stroke Belt, known for its persistent high relative excess of stroke mortality. Despite counties in the Stroke Belt having similar stroke severity, this area is also mixed by the two clusters, with proportions of 70% and 30%, respectively.

These results suggest that regions sharing similar geographic and stroke characteristics may have very different SDOH-stroke mortality associations, and we may need to consider separating two types of policies for the SDOH adjustments in stroke management based on our clustering results.

In addition, we illustrate the selected 18 covariates of SDOH in Table 2, ordered by their relative importance (Grömping, 2007) defined as

$$\text{RI}(\beta_{j\cdot}) = \|\beta_{j\cdot}\|_2 \left\{ \frac{1}{n} \sum_{i=1}^n \|X_{ij} - \frac{1}{n} \sum_{i=1}^n X_{ij}\|^2 \right\}^{1/2}.$$

We find that the influence of the SDOH on stroke mortality is mainly contributed by four aspects: social environment, built environment, health care system, and biology. Beyond the well-studied determinants from economic, cultural, and racial domains (Tsao et al., 2023), we find that stroke mortality is significantly associated with living and working environments, education level, and overuse of opioids. Typically, among the selected variables of SDOH, most of them are related to economic development. For example, in Table 2, MEDIAN_HOME_VALUE may reflect overall economic development and infrastructure building in the community. Additionally, a higher value of ELDERLY_RENTER may suggest a larger elderly population with lower income, facing issues such as housing instability. These economic-related factors may be potentially addressed through more equitable economic policies. For example, MEDIAN_HOME_VALUE can be adjusted by facilitating economic development. In addition, serving as a sign of the elderly living condition, ELDERLY_RENTER can be adjusted by improving elderly welfare.

To further quantify the longitudinal associations between SDOH and stroke mortality, we investigate the functional coefficients β_{jk} estimated from the dataset. Here, we only focus on the coefficients from the leading four important SDOH, which are ME-

DIAN_HOME_VALUE, NO_ENGLISH, ASIAN_LANG, and ELDERLY_RENTER. Their longitudinal associations in the two clusters are shown in Figure 5, along with their 95% confidence bands obtained by bootstraps. We notice that the leading four SDOH possess time-varying associations with stroke mortality, which are distinguished by two clusters. Furthermore, these associations are notably different between the two clusters. For example, the fluctuation of the longitudinal associations in cluster 2 is more significant than those in cluster 1. Additionally, we observe that in cluster 2, all four associations exhibit a common inflection point in 2013 (the dotted vertical lines in Figure 5). These findings help us better understand the dynamics of the associations between SDOH and stroke mortality in US counties.

In Figure 5, MEDIAN_HOME_VALUE shows a stable and weak association with stroke mortality for the counties in cluster 1, while those in cluster 2 exhibit a more intense negative effect with stroke mortality. The situation for ELDERLY_RENTER differs, with the association in cluster 2 showing significant fluctuation, while that in cluster 1 presents a time-increasing negative association with stroke mortality. Typically, economic factors have been found to affect stroke outcomes causally (Bann et al., 2023). As two economic-related factors, MEDIAN_HOME_VALUE and ELDERLY_RENTER have also been identified to possess significant associations with stroke mortality (Rodgers et al., 2019; Mawhorter et al., 2023). Our findings not only align with existing literature but also provide further insights into more tailored stroke mortality prevention strategies related to SDOH variables. For instance, the notable negative association between MEDIAN_HOME_VALUE and stroke mortality in cluster 2 highlights the importance of focusing on infrastructure development, maintenance, and enhancing overall economic equity in these regions. Noting the time-increasing negative association between ELDERLY_RENTER and stroke mortal-

ity in cluster 1, it may be beneficial to prioritize viable housing programs for lower-income elderly populations in these regions. Initiatives such as housing vouchers or subsidies may also be helpful, particularly in recent years when inflation is on the rise.

In addition to the above two covariates, `NO_ENGLISH` and `ASIAN_LANG` are two other SDOH variables measuring the sociocultural environment of the county. `NO_ENGLISH`, an indicator of the percentage of the population that does not speak English at all, is found to be associated with stroke mortality in both clusters. The direction of the associations shifts from positive to negative. A similar decreasing trend is observed in the association between `ASIAN_LANG` (a measure of the percentage of the population that speaks Asian and Pacific Island languages) and stroke mortality in cluster 2. Meanwhile, the association between `ASIAN_LANG` and stroke mortality in cluster 1 remains stable and weakly positive over time.

Our result shows that the association between the density of immigrants or Asian and Pacific Islanders and stroke mortality may not be uniform across regions and time periods. It is worth considering that immigrants or Asian and Pacific Islanders who experience a stroke may encounter challenges in accessing timely stroke care if they do not speak English. This language barrier may potentially contribute to an increased risk of stroke-related death in specific regions and during certain time periods (Shah et al., 2015). However, as suggested by our results, their risks with stroke-related death may have diminished from 2010 to 2018. This implies a gradual improvement of stroke care for immigrants or Asian and Pacific Islanders in the US, particularly for the counties in cluster 2.

5 Discussion

In this article, we introduce a novel clustering method for regional divisions of US counties based on their longitudinal associations between SDOH and stroke mortality. The challenges for this task arise from the latent and cluster-specific nature of the associations, which are compounded by their functional and high-dimensional characteristics simultaneously. To tackle these complex structures, we propose an REM algorithm that utilizes a finite mixture of functional linear concurrent models. Our method explores the clustering-invariant sparsity via a FGSCAD-Net penalty within the REM algorithm, allowing for efficient variable selection in the functional covariates to identify the most significant associations among all clusters. The effectiveness of our method has been demonstrated via extensive simulations. In the end, we apply the proposed method to our SDOH – stroke mortality longitudinal data, facilitating the regional divisions of US counties. This enables the identification of regions for informing SDOH-targeted prevention of stroke mortality.

In the analysis of the SDOH and stroke mortality dataset, our clustering map represents a novel result for region-division in stroke management, taking into account the similarity among the longitudinal associations between SDOH and stroke mortality. These findings suggest that heterogeneity in the associations occurs even within areas sharing similar geographical conditions, stroke mortality, or economic status. This implies that the region divisions solely based on the above factors may not be effective for SDOH-based stroke death control. Moreover, we uncover various patterns of longitudinal associations among the two identified clusters in US counties. The dynamics within these associations, including scale, trends, and inflection points, not only provide heuristic information for understanding complex SDOH – stroke mortality associations but are also useful for establishing timely SDOH adjustments in stroke death control. Finally, the proposed clustering method can

also be generalized to other high-dimensional longitudinal datasets, serving for clustering and variable selections in their longitudinal associations.

SUPPLEMENTARY MATERIAL

“SuppMaterial.pdf”: This file describes the details related to the proposed approach method, including the dataset, the selection scheme of tuning parameters, and other supporting results of the simulation study.

References

- Bann, D., L. Wright, A. Hughes, and N. Chaturvedi (2023). Socioeconomic inequalities in cardiovascular disease: a causal perspective. *Nature Reviews Cardiology*, 1–12.
- Benjamin, E. J., P. Muntner, A. Alonso, M. S. Bittencourt, C. W. Callaway, A. P. Carson, A. M. Chamberlain, A. R. Chang, S. Cheng, S. R. Das, et al. (2019). Heart disease and stroke statistics—2019 update: a report from the american heart association. *Circulation* 139(10), e56–e528.
- Breheny, P. and J. Huang (2015). Group descent algorithms for nonconvex penalized linear and logistic regression models with grouped predictors. *Statistics and computing* 25(2), 173–187.
- Cai, T. T., J. Ma, and L. Zhang (2019). Chime: Clustering of high-dimensional gaussian mixtures with em algorithm and its optimality. *The Annals of Statistics* 47(3), 1234–1267.
- Fan, J. and R. Li (2001). Variable selection via nonconcave penalized likelihood and its oracle properties. *Journal of the American statistical Association* 96(456), 1348–1360.
- Gebreab, S. Y., S. K. Davis, J. Symanzik, G. A. Mensah, G. H. Gibbons, and A. V. Diez-Roux (2015). Geographic variations in cardiovascular health in the united states: contributions of state-and individual-level factors. *Journal of the American Heart Association* 4(6), e001673.

- Goldsmith, J. and J. E. Schwartz (2017). Variable selection in the functional linear concurrent model. Statistics in medicine 36(14), 2237–2250.
- Grömping, U. (2007). Relative importance for linear regression in r: the package relaimpo. Journal of statistical software 17, 1–27.
- Havranek, E. P., M. S. Mujahid, D. A. Barr, I. V. Blair, M. S. Cohen, S. Cruz-Flores, G. Davey-Smith, C. R. Dennison-Himmelfarb, M. S. Lauer, D. W. Lockwood, et al. (2015). Social determinants of risk and outcomes for cardiovascular disease: a scientific statement from the american heart association. Circulation 132(9), 873–898.
- He, J., Z. Zhu, J. D. Bundy, K. S. Dorans, J. Chen, and L. L. Hamm (2021). Trends in cardiovascular risk factors in us adults by race and ethnicity and socioeconomic status, 1999-2018. Jama 326(13), 1286–1298.
- Holloway, R. G., R. M. Arnold, C. J. Creutzfeldt, E. F. Lewis, B. J. Lutz, R. M. McCann, A. A. Rabinstein, G. Saposnik, K. N. Sheth, D. B. Zahuranec, et al. (2014). Palliative and end-of-life care in stroke: a statement for healthcare professionals from the american heart association/american stroke association. Stroke 45(6), 1887–1916.
- Huang, J. Z., H. Shen, and A. Buja (2009). The analysis of two-way functional data using two-way regularized singular value decompositions. Journal of the American Statistical Association 104(488), 1609–1620.
- Jacobs, R. A., M. I. Jordan, S. J. Nowlan, and G. E. Hinton (1991). Adaptive mixtures of local experts. Neural computation 3(1), 79–87.
- Jacques, J. and C. Preda (2013). Funclust: A curves clustering method using functional random variables density approximation. Neurocomputing 112, 164–171.
- Jacques, J. and C. Preda (2014). Model-based clustering for multivariate functional data. Computational Statistics & Data Analysis 71, 92–106.

- Jiang, W. and M. A. Tanner (1999). Hierarchical mixtures-of-experts for exponential family regression models: approximation and maximum likelihood estimation. The Annals of Statistics 27(3), 987–1011.
- Kapral, M. K., P. C. Austin, G. Jeyakumar, R. Hall, A. Chu, A. M. Khan, A. Y. Jin, C. Martin, D. Manuel, F. L. Silver, et al. (2019). Rural-urban differences in stroke risk factors, incidence, and mortality in people with and without prior stroke: The canheart stroke study. Circulation: Cardiovascular Quality and Outcomes 12(2), e004973.
- Khalili, A. and J. Chen (2007). Variable selection in finite mixture of regression models. Journal of the American Statistical Association 102(479), 1025–1038.
- Kong, D., K. Xue, F. Yao, and H. H. Zhang (2016). Partially functional linear regression in high dimensions. Biometrika 103(1), 147–159.
- Koton, S., A. L. Schneider, W. D. Rosamond, E. Shahar, Y. Sang, R. F. Gottesman, and J. Coresh (2014). Stroke incidence and mortality trends in us communities, 1987 to 2011. Jama 312(3), 259–268.
- Kowarik, A. and M. Templ (2016). Imputation with the r package vim. Journal of statistical software 74, 1–16.
- Labarthe, D., B. Grover, J. Galloway, L. Gordon, S. Moffatt, T. Pearson, M. Schoeberl, and S. Sidney (2014). The public health action plan to prevent heart disease and stroke: Ten-year update. In Washington, DC: National Forum for Heart Disease and Stroke Prevention.
- Li, G., H. Shen, and J. Z. Huang (2016). Supervised sparse and functional principal component analysis. Journal of Computational and Graphical Statistics 25(3), 859–878.
- Liang, D., H. Zhang, X. Chang, and H. Huang (2021). Modeling and regionalization of china’s pm_{2.5} using spatial-functional mixture models. Journal of the American Statistical Association 116(533), 116–132.

- Lu, Z. and X. Song (2012). Finite mixture varying coefficient models for analyzing longitudinal heterogenous data. Statistics in medicine 31(6), 544–560.
- Mawhorter, S., E. M. Crimmins, and J. A. Ailshire (2023). Housing and cardiometabolic risk among older renters and homeowners. Housing studies 38(7), 1342–1364.
- Meier, L., S. Van de Geer, and P. Bühlmann (2009). High-dimensional additive modeling. The Annals of Statistics 37(6B), 3779–3821.
- Mozaffarian, D., E. J. Benjamin, A. S. Go, D. K. Arnett, M. J. Blaha, M. Cushman, S. De Ferranti, J.-P. Després, H. J. Fullerton, V. J. Howard, et al. (2015). Heart disease and stroke statistics—2015 update: a report from the american heart association. circulation 131(4), e29–e322.
- Powell-Wiley, T. M., Y. Baumer, F. O. Baah, A. S. Baez, N. Farmer, C. T. Mahlobo, M. A. Pita, K. A. Potharaju, K. Tamura, and G. R. Wallen (2022). Social determinants of cardiovascular disease. Circulation research 130(5), 782–799.
- Ramsay, J. and B. Silverman (2005). Functional Data Analysis (2nd ed.). Springer.
- Ramsay, J. O. and B. W. Silverman (2002). Applied functional data analysis: methods and case studies. Springer.
- Rand, W. M. (1971). Objective criteria for the evaluation of clustering methods. Journal of the American Statistical association 66(336), 846–850.
- Record, N. B., D. K. Onion, R. E. Prior, D. C. Dixon, S. S. Record, F. L. Fowler, G. R. Cayer, C. I. Amos, and T. A. Pearson (2015). Community-wide cardiovascular disease prevention programs and health outcomes in a rural county, 1970-2010. Jama 313(2), 147–155.
- Rodgers, J., B. A. Briesacher, R. B. Wallace, I. Kawachi, C. F. Baum, and D. Kim (2019). County-level housing affordability in relation to risk factors for cardiovascular disease among

- middle-aged adults: The national longitudinal survey of youths 1979. Health & place 59, 102194.
- Shah, B. R., N. A. Khan, M. J. O'Donnell, and M. K. Kapral (2015). Impact of language barriers on stroke care and outcomes. Stroke 46(3), 813–818.
- Son, H., D. Zhang, Y. Shen, A. Jaysing, J. Zhang, Z. Chen, L. Mu, J. Liu, J. Rajbhandari-Thapa, Y. Li, et al. (2023). Social determinants of cardiovascular health: a longitudinal analysis of cardiovascular disease mortality in us counties from 2009 to 2018. Journal of the American Heart Association 12(2), e026940.
- Tsao, C. W., A. W. Aday, Z. I. Almarzooq, A. Alonso, A. Z. Beaton, M. S. Bittencourt, A. K. Boehme, A. E. Buxton, A. P. Carson, Y. Commodore-Mensah, et al. (2022). Heart disease and stroke statistics—2022 update: a report from the american heart association. Circulation 145(8), e153–e639.
- Tsao, C. W., A. W. Aday, Z. I. Almarzooq, C. A. Anderson, P. Arora, C. L. Avery, C. M. Baker-Smith, A. Z. Beaton, A. K. Boehme, A. E. Buxton, et al. (2023). Heart disease and stroke statistics—2023 update: a report from the american heart association. Circulation 147(8), e93–e621.
- Villablanca, A. C., C. Slee, L. Lianov, and D. Tancredi (2016). Outcomes of a clinic-based educational intervention for cardiovascular disease prevention by race, ethnicity, and urban/rural status. Journal of Women's Health 25(11), 1174–1186.
- Wang, L., H. Li, and J. Z. Huang (2008). Variable selection in nonparametric varying-coefficient models for analysis of repeated measurements. Journal of the American Statistical Association 103(484), 1556–1569.
- Yao, F., Y. Fu, and T. C. Lee (2011). Functional mixture regression. Biostatistics 12(2), 341–353.

- Yi, X. and C. Caramanis (2015). Regularized em algorithms: A unified framework and statistical guarantees. Advances in Neural Information Processing Systems 28.
- Zelko, A., P. R. Salerno, S. Al-Kindi, F. Ho, F. P. Rocha, K. Nasir, S. Rajagopalan, S. Deo, and N. Sattar (2023). Geographically weighted modeling to explore social and environmental factors affecting county-level cardiovascular mortality in people with diabetes in the united states: A cross-sectional analysis. The American Journal of Cardiology 209, 193–198.
- Zeng, L. and J. Xie (2014). Group variable selection via scad-l 2. Statistics 48(1), 49–66.
- Zou, H. and T. Hastie (2005). Regularization and variable selection via the elastic net. Journal of the royal statistical society: series B (statistical methodology) 67(2), 301–320.
- Zou, H. and H. H. Zhang (2009). On the adaptive elastic-net with a diverging number of parameters. Annals of statistics 37(4), 1733.

List of Figures

1	The correlation matrix for the SDOH variables (indexed by numbers). The correlation of the longitudinal data between the j th SDOH and j' th SDOH is calculated as $C_{j,j'} / \sqrt{C_{j,j}C_{j',j'}}$, where $C_{j,j'} = n^{-1} \sum_{i=1}^n S_i^{-1} \sum_{s=1}^{S_i} \{X_{ij}(t_{is}) - \hat{\mu}_j(t_{is})\} \{X_{ij'}(t_{is}) - \hat{\mu}_{j'}(t_{is})\}$ with $\hat{\mu}_j(\cdot)$ being the estimated mean function for the j th county. Here, $X_{ij}(t_{is})$ is the observed data of the j th SDOH at the i th county on year t_{is} , for $i = 1, \dots, n$, $j = 1, \dots, p$, and $s = 1, \dots, S_i$. The definition of $X_{ij}(t_{is})$, n , p , and S_i can be found in Section 2.2.	34
2	State-wise and rural-urban Pearson correlations between the stroke mortality and PAPL. Panels (A) and (C) are the geographical maps of correlations for the years 2009, 2013, and 2018, respectively for two types of division strategies. Panels (B) and (D) are the state-wise and rural-urban longitudinal correlations from 2009 – 2018, respectively.	35
3	The true curves of the functional coefficients β_{jk} from each cluster k and their estimations for $n = 180$, $p = 240$, and $\alpha = 0.8$. The solid black line represents the true curve, while the solid red, green, and blue lines, along with their corresponding bands, represent the pointwise means and the 95% confidence bands over 100 replicated simulations.	36
4	The clustering result for the county-level longitudinal associations between the SDOH and stroke mortality in the US. The regions in grey color represent the area without available data.	37
5	The estimated longitudinal associations for the leading four SDOH in two clusters. The dotted horizontal line in each sub-figure represents the zero line for the SDOH-stroke mortality longitudinal associations, and the dotted vertical line in each sub-figure indicates the common reflection point of the longitudinal associations in cluster 2.	38

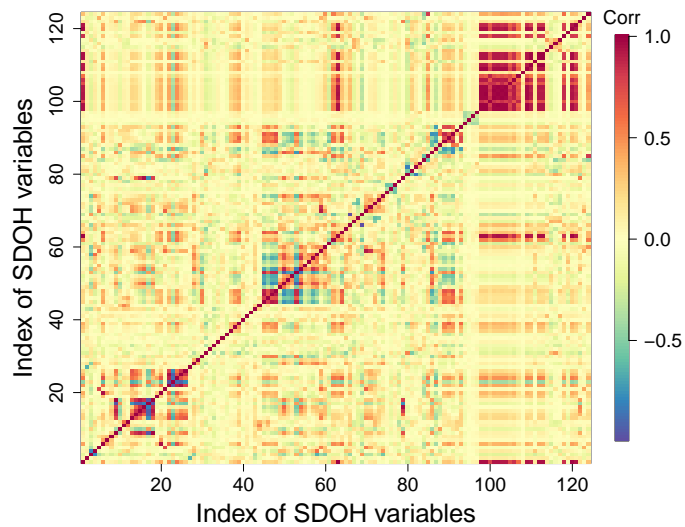


Figure 1: The correlation matrix for the SDOH variables (indexed by numbers). The correlation of the longitudinal data between the j th SDOH and j' th SDOH is calculated as $C_{j,j'}/\sqrt{C_{j,j}C_{j',j'}}$, where $C_{j,j'} = n^{-1} \sum_{i=1}^n S_i^{-1} \sum_{s=1}^{S_i} \{X_{ij}(t_{is}) - \hat{\mu}_j(t_{is})\} \{X_{ij'}(t_{is}) - \hat{\mu}_{j'}(t_{is})\}$ with $\hat{\mu}_j(\cdot)$ being the estimated mean function for the j th county. Here, $X_{ij}(t_{is})$ is the observed data of the j th SDOH at the i th county on year t_{is} , for $i = 1, \dots, n$, $j = 1, \dots, p$, and $s = 1, \dots, S_i$. The definition of $X_{ij}(t_{is})$, n , p , and S_i can be found in Section 2.2.

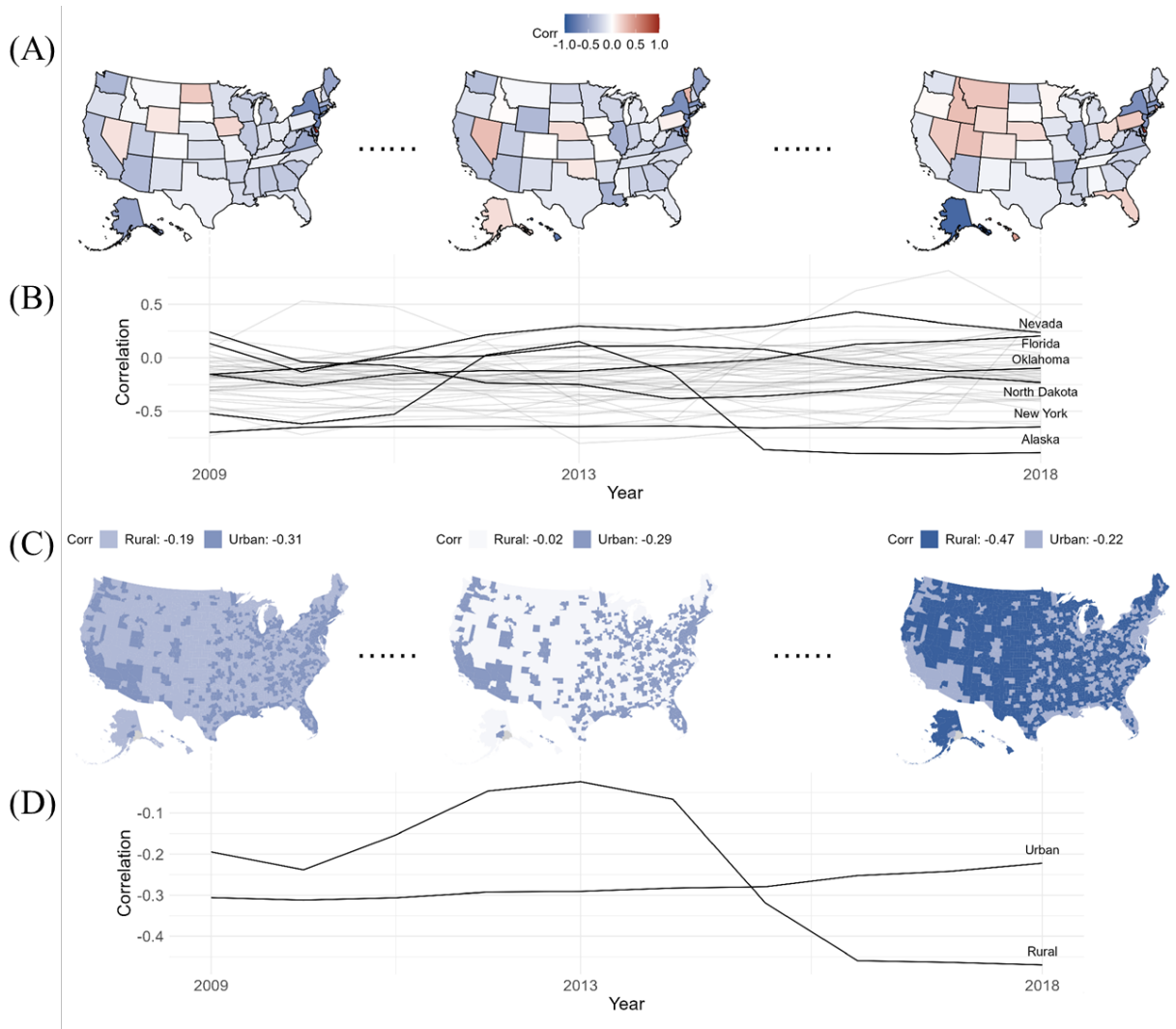


Figure 2: State-wise and rural-urban Pearson correlations between the stroke mortality and PAPL. Panels (A) and (C) are the geographical maps of correlations for the years 2009, 2013, and 2018, respectively for two types of division strategies. Panels (B) and (D) are the state-wise and rural-urban longitudinal correlations from 2009 – 2018, respectively.

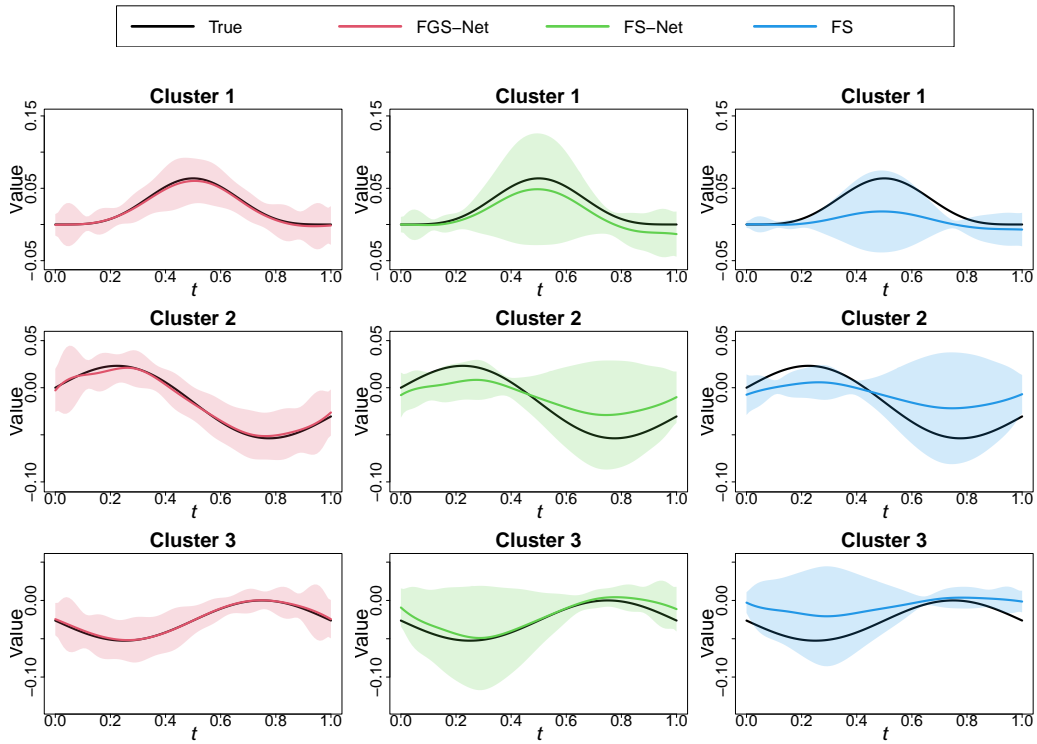


Figure 3: The true curves of the functional coefficients β_{jk} from each cluster k and their estimations for $n = 180$, $p = 240$, and $\alpha = 0.8$. The solid black line represents the true curve, while the solid red, green, and blue lines, along with their corresponding bands, represent the pointwise means and the 95% confidence bands over 100 replicated simulations.

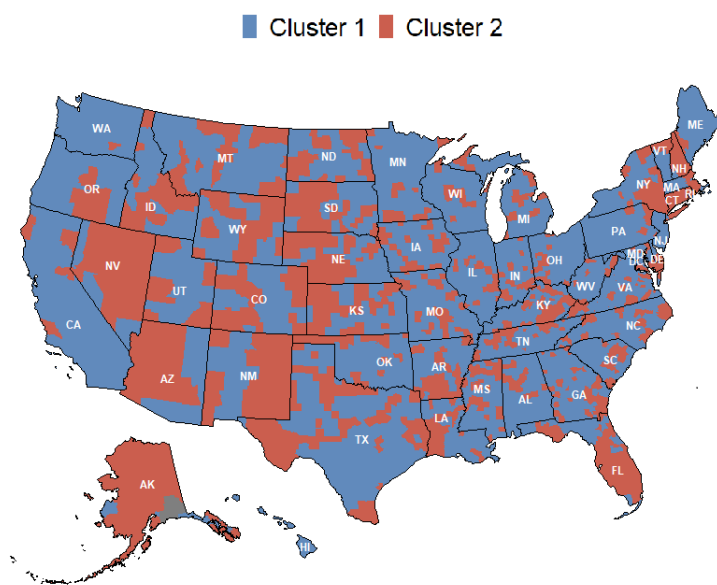


Figure 4: The clustering result for the county-level longitudinal associations between the SDOH and stroke mortality in the US. The regions in grey color represent the area without available data.

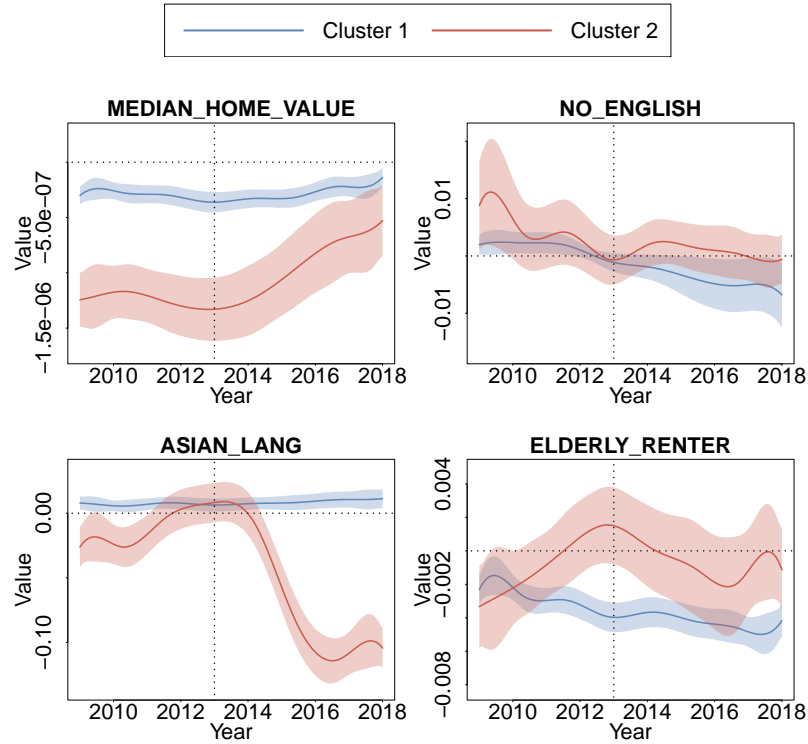


Figure 5: The estimated longitudinal associations for the leading four SDOH in two clusters. The dotted horizontal line in each sub-figure represents the zero line for the SDOH-stroke mortality longitudinal associations, and the dotted vertical line in each sub-figure indicates the common reflection point of the longitudinal associations in cluster 2.

List of Tables

1	Averaged ARI, C, IC, and MSE for FGS-Net, FS-Net, FS, RP, VS-RP, and LI-MIX with $p = 10, n/6, n/2, 4n/3$, $\alpha = 0.4, 0.8$, $n = 180, 300$. The highest ARI, C, and lowest IC, MSE are in bold.	40
2	The selected SDOH variables ranked by descent order of their relative importance.	41

Table 1: Averaged ARI, C, IC, and MSE for FGS-Net, FS-Net, FS, RP, VS-RP, and LI-MIX with $p = 10, n/6, n/2, 4n/3$, $\alpha = 0.4, 0.8$, $n = 180, 300$. The highest ARI, C, and lowest IC, MSE are in bold.

		$n = 180$															
		$p=10$				$p=30$				$p=100$				$p=240$			
Model		ARI	C	IC	MSE	ARI	C	IC	MSE	ARI	C	IC	MSE	ARI	C	IC	MSE
$\alpha = 0.4$	Truth	1	12	0	0	1	72	0	0	1	252	0	0	1	702	0	0
	RP	1.00	0.00	0.00	0.04	0.01	0.00	0.00	1.00	0.00	0.00	0.00	1.00	0.01	0.00	0.00	1.00
	VS-RP	0.45	11.94	8.82	0.70	0.43	71.70	8.85	0.72	0.39	251.34	9.06	0.76	0.33	700.23	9.09	0.79
	LI-MIX	0.28	4.89	2.31	0.72	0.23	37.05	2.52	0.79	0.06	125.88	2.97	1.35	0.01	370.83	3.12	2.81
	FS	1.00	12.00	0.06	0.03	1.00	72.00	0.00	0.03	0.97	251.93	0.45	0.09	0.93	701.86	1.09	0.13
	FS-Net	1.00	12.00	0.07	0.03	1.00	72.00	0.00	0.02	0.97	251.96	0.50	0.09	0.94	701.93	0.96	0.12
	FGS-Net	1.00	12.00	0.00	0.03	1.00	72.00	0.00	0.02	0.99	252.00	0.00	0.05	0.98	702.00	0.18	0.08
$\alpha = 0.8$	Truth	1	12	0	0	1	72	0	0	1	252	0	0	1	702	0	0
	RP	1.00	0.00	0.00	0.08	0.01	0.00	0.00	0.99	0.01	0.00	0.00	1.00	0.01	0.00	0.00	1.00
	VS-RP	0.86	11.73	9.60	0.82	0.85	71.31	9.54	0.82	0.84	251.22	9.87	0.85	0.81	699.75	11.22	0.97
	LI-MIX	0.22	6.15	4.05	0.87	0.18	42.60	4.29	1.05	0.08	150.27	4.35	1.85	0.02	437.73	4.38	5.15
	FS	1.00	11.92	1.42	0.19	1.00	70.60	1.82	0.22	0.98	248.59	3.35	0.36	0.97	701.91	8.51	0.77
	FS-Net	1.00	11.91	0.34	0.11	1.00	70.88	0.48	0.12	0.98	249.85	1.36	0.21	0.98	701.92	6.41	0.55
	FGS-Net	1.00	12.00	0.03	0.09	1.00	72.00	0.03	0.09	0.98	251.97	0.21	0.15	0.99	701.91	0.72	0.16
		$n = 300$															
		$p=10$				$p=50$				$p=150$				$p=400$			
Model		ARI	C	IC	MSE	ARI	C	IC	MSE	ARI	C	IC	MSE	ARI	C	IC	MSE
$\alpha = 0.4$	Truth	1	12	0	0	1	132	0	0	1	432	0	0	1	1182	0	0
	RP	1.00	0.00	0.00	0.04	0.01	0.00	0.00	1.00	0.01	0.00	0.00	1.00	0.01	0.00	0.00	1.00
	VS-RP	0.83	11.97	6.21	0.42	0.82	131.73	6.36	0.43	0.82	431.34	6.45	0.43	0.85	1179.78	5.82	0.39
	LI-MIX	0.33	4.56	0.96	1.12	0.27	63.45	1.11	1.18	0.10	229.26	1.29	1.44	0.01	648.66	1.50	2.90
	FS	0.99	12.00	0.06	0.03	1.00	132.00	0.00	0.01	1.00	432.00	0.00	0.01	0.99	1181.97	0.06	0.04
	FS-Net	0.99	12.00	0.06	0.03	1.00	132.00	0.00	0.01	1.00	432.00	0.00	0.01	0.99	1181.97	0.06	0.03
	FGS-Net	0.99	12.00	0.00	0.05	1.00	132.00	0.00	0.01	1.00	432.00	0.00	0.04	0.99	1182.00	0.00	0.02
$\alpha = 0.8$	Truth	1	12	0	0	1	132	0	0	1	432	0	0	1	1182	0	0
	RP	1.00	0.00	0.00	0.07	0.01	0.00	0.00	0.99	0.01	0.00	0.00	1.00	0.01	0.00	0.00	1.00
	VS-RP	0.91	11.76	9.12	0.76	0.91	131.10	9.18	0.78	0.89	429.78	9.06	0.77	0.87	1176.21	9.18	0.79
	LI-MIX	0.24	6.87	3.36	1.14	0.19	77.67	3.27	1.28	0.09	261.63	3.15	1.79	0.02	768.21	3.66	4.08
	FS	0.99	11.99	0.25	0.09	0.98	131.69	0.33	0.09	1.00	430.90	0.05	0.06	0.96	1181.96	8.05	0.75
	FS-Net	0.99	12.00	0.09	0.06	0.99	131.74	0.20	0.08	1.00	431.13	0.02	0.05	0.97	1181.95	5.90	0.50
	FGS-Net	0.99	12.00	0.06	0.09	0.99	132.00	0.09	0.07	0.99	432.00	0.06	0.09	0.99	1182.00	0.66	0.12

Table 2: The selected SDOH variables ranked by descent order of their relative importance.

Variable	Explanation	SDOH Domain
MEDIAN_HOME.VALUE	Median home value of owner-occupied housing units	Sociocultural Environment
NO_ENGLISH	Population that does not speak English at all, %	Sociocultural Environment
ASIAN_LANG	Population that speaks Asian and Pacific Island languages, %	Sociocultural Environment
ELDERLY_RENTER	Rental units occupied by householders aged 65 and older, %	Built Environment
GINIINDEX	Gini index of income inequality	Sociocultural Environment
HOME_WITH_KIDS	Owner-occupied housing units with children, %	Built Environment
AGRI_JOB	Employed working in agriculture, forestry, fishing and hunting, and mining, %	Sociocultural Environment
NO_VEHICLE	Housing units with no vehicle available, %	Built Environment
OPIOID	Number of opioid prescriptions per 100 persons	Health Care System
WEAK_ENGLISH	Population that does not speak English well, %	Sociocultural Environment
BLACK	Population reporting Black race, %	Biology
BACHELOR	Population with a bachelor's degree, %	Sociocultural Environment
NO_FUEL_HOME	Occupied housing units without fuel, %	Built Environment
TIME	Time Effect	Sociocultural Environment
ONLY_ENGLISH	Population that only speaks English, %	Sociocultural Environment
MOBILE_HOME	Housing units that are mobile homes, %	Built Environment
BELOW_HIGH_SCH	Population with less than high school education, %	Sociocultural Environment
DRIVE_2WORK	Workers taking a car, truck, or van to work, %	Built Environment